Mol. Cells 2014; 37(4): 314-321
http://dx.doi.org/10.14348/molcells.2014.2360

Molecules and Cells
http://molcells.org
Established in 1990

Inhibition of Cell Proliferation and Migration by miR-509-3p That Targets CDK2, Rac1, and PIK3C2A

Sena Yoon[1,2], Eunji Han[1,2], Young-Chul Choi[1,2], Honghwan Kee[1], Yongsu Jeong[1], Jaeseung Yoon[1], and Kwanghee Baek[1,*]

CDK2 is a key regulator of cell cycle progression. In this study, we screened for miRNAs targeting CDK2 using a luciferase-3′-untranslated region reporter assay. Among 11 hit miRNAs, miR-509-3p reduced CDK2 protein levels and significantly inhibited cancer cell growth. Microarray, Western blotting, and luciferase reporter analyses revealed additional targets of miR-509-3p, including Rac1 and PIK3C2A. Overexpression of miR-509-3p induced G1 cell-cycle arrest and inhibited colony formation and migration. RNAi experiments indicated that the growth-inhibitory effects of miR-509-3p may occur through down-regulation of CDK2, Rac1, and PIK3C2A. Targeting of multiple growth regulatory genes by miR-509-3p may contribute to effective anti-cancer therapy.

INTRODUCTION

MicroRNAs (miRNAs) are small non-coding RNAs that regulate the expression of many genes by binding to the 3′-untranslated region (3′-UTR) of target mRNAs (Bartel, 2004; He and Hannon, 2004). Increasing evidence shows that miRNAs play important roles in various physiological and pathological processes. In cancer, miRNAs can function as oncogenes or tumor suppressors to either promote or protect against cancer, respectively. (Hoshino and Matsubara, 2013). The most well-characterized tumor suppressor miRNAs are miR-15a, miR-16-1, miR-34, and the let-7 family (Aqeilan et al., 2010; Büssing et al., 2008; Hermeking, 2010). In the case of miR-34, several tens of genes have been validated as direct targets, and the suppression of cancer-promoting target genes *en bloc* may efficiently inhibit the uncontrollable growth of cancer cells by inducing apoptosis, cell cycle arrest, and senescence (Bader, 2012). Recently, it was reported that miR-509-3p may function as a tumor suppressor in renal cancer (Zhai et al., 2012). The expression level of miR-509-3p is lower in renal cancer than in the adjacent normal tissues and ectopic expression of miR-509-3p inhibits renal cell growth and migration. To date, the target genes and the mechanism by which miR-509-3p suppresses cell proliferation remain unclear.

Cyclin-dependent kinase 2 (CDK2) is a serine/threonine kinase that controls the cell cycle by forming a complex with a regulatory subunit, that is, cyclin E or A. Although CDK2 plays an important role in G1/S transition and S-phase progression, knockout experiments indicate that CDK2 is not essential for normal mouse development, except for the meiotic division of male and female germ cells (Ortega et al., 2003). However, inhibition of CDK2 activity by using dominant-negative forms of CDK2, microinjection of antibodies against CDK2, or overexpression of $p27^{Kip1}$ has been shown to block cell cycle progression (Hu et al., 2001; Tsai et al., 1993; Wang et al., 1997). Moreover, knockdown of CDK2 using siRNA suppresses cell proliferation and induces apoptosis in several cancer cell lines, although exceptions exist (Faber and Chiles, 2007; Long et al., 2010; Tetsu and McCormick, 2003). The effect of CDK2 inactivation on cell cycle progression may vary depending on the cell types used in *in vitro* and *in vivo* experiments.

In this study, we found that miR-509-3p directly targets CDK2, Ras-related C3 botulinum toxin substrate 1 (Rac1), and phosphatidylinositol-4-phosphate 3-kinase catalytic subunit type 2 alpha (PIK3C2A). As revealed by siRNA-based gene silencing, down-regulation of CDK2, Rac1, and PIK3C2A may account for the inhibitory effects of miR-509-3p on cell proliferation, colony formation, and migration.

MATERIALS AND METHODS

RNA oligonucleotides

MicroRNA mimics, siRNAs, and a negative control (NC) were purchased from Shanghai GenePharma Company (China). The 19-mer target sequence of siRNAs is shown in Supplementary Table 1.

Cell lines and transfection

Human cell line A549 (human epithelial, lung carcinoma de-

[1]Graduate School of Biotechnology, Kyung Hee University, Yongin 446-701, Korea, [2]These authors contributed equally to this work.
*Correspondence: khbaek@khu.ac.kr

Received 2 December, 2013; revised 7 March, 2014; accepted 11 March, 2014; published online 21 April, 2014

Keywords: CDK2, growth inhibition, microRNA, miR-509-3p, PIK3C2A, Rac1

eISSN: 0219-1032

rived; KCLB 10185), HeLa (human epithelial, cervix adenocarcinoma derived, KCLB 10002), KB (human epithelial, HeLa contaminant, KCLB 10017), and NCI-H460 (human epithelial, lung carcinoma derived, KCLB 30177) were obtained from Korean Cell Line Bank (Korea). Cells were cultured in RPMI-1640 supplemented with 10% fetal bovine serum in a humidified atmosphere containing 5% CO_2 at 37°C. WI-38 (human fibroblast derived from normal embryonic lung tissue) was obtained from the American Type Culture Collection (USA) and cultured in ATCC-formulated Eagle's Minimum Essential Medium supplemented with 10% heat-inactivated fetal bovine serum. Transfection was performed using Lipofectamine RNAiMAX (Invitrogen) according to manufacturer's protocol as described previously (Kim et al., 2008).

Construction of luciferase-3′-UTR reporter plasmids and luciferase assay

The full-length cDNA clones containing the 3′-UTR of CDK2 (NM_001798), Rac1 (NM_006908), and PIK3C2A (NM_002645) genes were obtained from Open Biosystems (USA). The 3′-UTR of CDK2, Rac1, and PIK3C2A was amplified by PCR using the following primers: (1) The sequence between 1136 and 1909 nt of CDK2 using primers CDK2-F and CDK2-R, (2) The sequence between 821 and 1320 nt of Rac1 using primers RAC1-F and RAC1-R, (3) The sequence between 5582 and 6891 nt of PIK3C2A using primers PIK3C2A-F and PIK3C2A-R. The amplified 3′-UTR sequences were cloned into XhoI/NotI sites of psiCHECK-2 vector (Promega) to give rise to luciferase-3′-UTR reporter plasmids. To delete predicted target sites of miR-509-3p from reporter plasmids, we used PCR approach as described previously (Kim et al., 2008). The location of binding sites for miR-509-3p in the 3′-UTR of CDK2, Rac1, and PIK3C2A is shown in Figs. 1D, 3D, and 3E, respectively, and the alignment of miR-509-3p with the target sites in the 3′-UTR of CDK2, Rac1, and PIK3C2A is shown in Supplementary Fig. 1. All primer sequences used to construct wild-type and mutant reporter plasmids are provided in Supplementary Table 2. For transfection and luciferase assay, Lipofectamine 2000 (Invitrogen) and Dual-Luciferase assay (Promega) were used respectively, following the manufacturer's protocol as described previously (Kim et al., 2008).

Western blot analysis

Western blotting was performed as described previously (Kim et al., 2008). Primary antibodies specific for CDK2 (#2546), YAP (#4912), PARP (#9542), Caspase 3 (#9662), and GAPDH (#2118) were obtained from Cell Signaling Technology (USA). The following antibodies were also used for immunoblotting: LC3B (NB100-2220, Novus Biologicals, USA), Rab5C (HPA003426, Sigma, USA), Rac1 (#610651, BD Transduction Laboratories, USA), PIK3C2A (sc-365290, Santa Cruz Biotechnology, USA), β-actin (C-11, Santa Cruz Biotechnology). GAPDH and β-actin antibodies were used as a loading control.

Quantitative real-time PCR analysis

Real-time PCR analysis was performed using the ABI Prism 7900 Sequence Detection System (Applied Biosystems) as described previously (Choung et al., 2006). Reaction mixtures (20 μl) contained 4 pmol of each primer and 2X SYBR Green PCR Master Mix (Applied Biosystems). PCR reaction was performed using the following conditions; initial denaturation at 50°C for 2 min and 95°C for 10 min followed by 40 cycles of 95°C for 30 s, 60°C for 30 s, and 72°C for 30 s. Primers specific for PIK3C2A (P292339) and Rab5C (P107690) were obtained from Bioneer (Korea). The sequences of the primers specific for LC3B were: forward primer, 5′-TTGGGAGTATCACAGGAAAA TC-3′; reverse primer, 5′-CCCGTTACAGTAAACAGCTTTC-3′. The sequences of the primers specific for Rac1 were: forward primer, 5′-TTG CCAAAATACCTTCTGAACT-3′; reverse primer, 5′-TGCTTTACGCATCTGAGAACTA-3′. The sequences of the primers specific for YAP1 were: forward primer, 5′-TTGTGAAT TAAAGTGGCACCAG-3′; reverse primer, 5′-AGGCTTTTCAT AGCAGCTTTTG-3′. Primers specific for GAPDH (GK-018) were obtained from GenoCheck (Korea). Normalized expression levels were obtained by dividing the amount of each cDNA by that of GAPDH.

Cell proliferation assay

For cell proliferation assay, A549 cells were seeded on 24-well plates at 1.8 x 10^4 cells per well. Next day, cells were transfected with miRNA mimics and siRNAs at 20 nM. At 72 h after transfection, cell proliferation was assessed using cell counting with a hemocytometer or Cell Counting Kit-8 (CCK-8; Japan) according to manufacturer's instructions.

Microarray experiments

Microarray analysis was performed using the Illumina HumanHT-12 v4 Expression BeadChip (Illumina, Inc., USA) as described previously (Kim et al., 2008). The array was scanned with the Illumina Bead Array Reader Confocal Scanner and data analysis was performed using the Illumina GenomeStudio v2009.2 (Gene Expression Module v1.5.4). The microarray data have been submitted to the Gene Expression Omnibus (GEO)/NCBI repository and assigned the accession number GSE47522.

Cell cycle analysis

A549 cells were transfected with miRNAs and siRNAs at a concentration of 20 nM. At 72 h post-transfection, cells were harvested and fixed with 70% ethanol. After fixation, cells were treated with RNase A (1 mg/ml) for 30 min and then, stained with propidium iodide (50 μg/ml). DNA content was analyzed using FACS Vantage SE flow cytometer (Becton Dickinson, USA).

Colony formation assay

At 24 h post-transfection, cells were harvested, counted, and seeded in 6-well plates at a density of 200 cells per well. After 10 days in culture, colonies were fixed with methanol and stained with 0.5% crystal violet in 25% methanol for 10 min at room temperature. The numbers of colonies containing more than 50 cells were counted in triplicate for each sample.

In vitro scratch assay

Transfected cells were grown to 100% confluence and a scratch was made by using a sterile 200 μl pipette tip. Cells were washed with PBS and incubated in complete culture medium. At 0, 12, and 24 h after wounding, images were taken using Leica DMI6000B microscope equipped with Leica DFC360 FX camera. Migration from the wound edge toward the wound area was measured by using Leica Application Suite version 3.8.0.

Statistical analysis

Data are shown as mean ± SD. The two-tailed Student's *t*-test was used to statistically analyze data between two groups. A P value less than 0.05 was considered statistically significant.

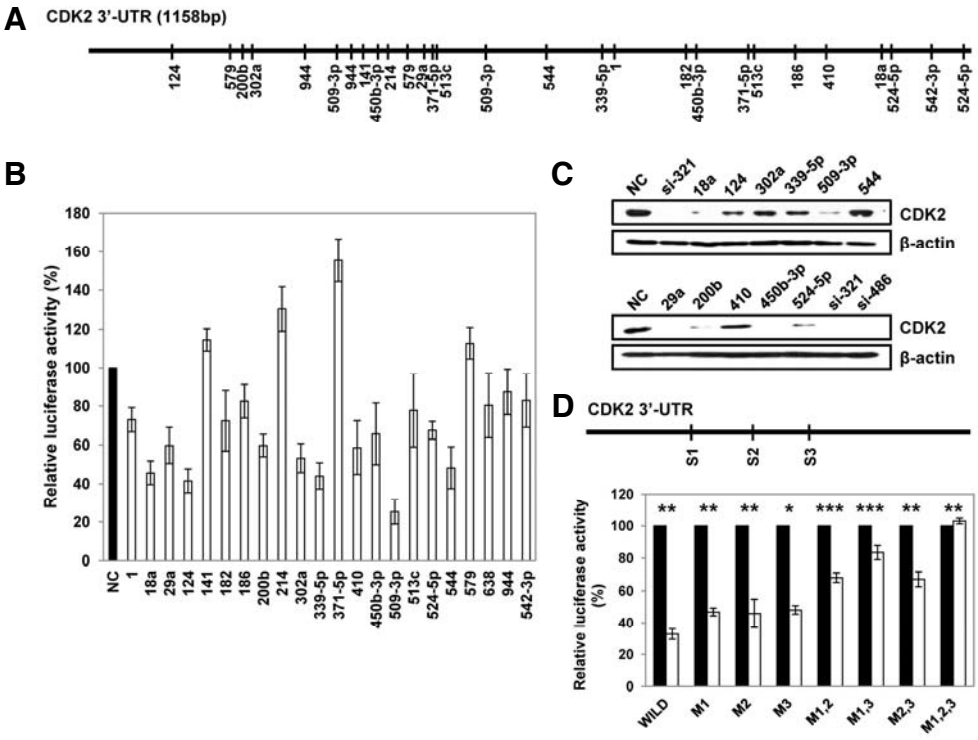

Fig. 1. Screening for miRNAs that target the 3′-UTR of CDK2. (A) The location of miRNAs predicted to target the 3′-UTR of CDK2 based on the TargetScan program. The binding site for miR-638 overlaps with that for miR-450b-3p. (B) Luciferase reporter assay. At 48 h after cotransfection with miRNA mimics (10 nM) and a luciferase-CDK2-3′-UTR reporter plasmid, luciferase activity was measured using a Dual-Luciferase assay (Promega). Normalized *Renilla* luciferase activity in cells transfected with NC was set at 100%. (C) A549 cells were transfected with miRNA mimics and siRNAs at 20 nM. At 48 h post-transfection, cells were subjected to Western blot analysis. si-321 and si-486 are siRNAs against CDK2. (D) Top: A schematic diagram of 3 binding sites (S1, S2, and S3) for miR-509-3p in the 3′-UTR of CDK2. The nucleotide positions of S1, S2, and S3 in the CDK2 gene are 1448, 1635, and 1805, respectively. Bottom: Direct targeting of the CDK2 3′-UTR by miR-509-3p. A549 cells were cotransfected with miRNA (10 nM) and luciferase reporter plasmids carrying the wild-type or mutated 3′-UTR of CDK2. The experiments were performed in triplicate and repeated thrice. $^{*}P < 0.001$, $^{**}P < 0.01$, $^{***}P < 0.05$. Filled bars, luciferase activity of NC-transfected cells; open bars, luciferase activity of miR-509-3p-transfected cells. Luciferase reporter plasmids cotransfected with NC or miR-509-3p are the following: WILD, wild-type 3′-UTR; M1, mutated at S1; M2, mutated at S2; M3, mutated at S3; M1,2, mutated at S1 and S2; M1,3, mutated at S1 and S3; M2,3, mutated at S2 and S3; M1,2,3, mutated at S1, S2, and S3.

RESULTS AND DISCUSSION

Identification of miRNAs targeting the 3′-UTR of CDK2 using a luciferase reporter assay

To identify miRNAs that regulate the expression of luciferase by targeting the 3′-UTR of CDK2, we constructed a luciferase reporter plasmid that contains the 3′-UTR of CDK2 downstream of the *Renilla* luciferase gene. Using the TargetScan prediction program, 22 miRNAs, including 2 miRNAs whose sites are conserved among vertebrates, were selected for screening (Fig. 1A). Each miRNA was cotransfected with a luciferase-3′-UTR reporter plasmid and luciferase activity was measured at 48 h post-transfection. As seen in Fig. 1B, a majority of the tested miRNAs down-regulated luciferase activity. Among them, 11 miRNAs reduced luciferase activity below 70% of that in NC-transfected cells, suggesting that these miRNAs negatively regulate gene expression *via* the 3′-UTR of CDK2. To validate CDK2 as a target of these miRNAs, the CDK2 protein level was examined by Western blot analysis. As shown in Fig. 1C, the protein level of CDK2 was significantly reduced by miR-18a, -29a, -124, -200b, -339-5p, -450b-3p, -509-3p, and -524-5p. These results indicate that CDK2 is a target of these 8 miRNAs, which down-regulate protein expression through the 3′-UTR of CDK2.

CDK2 is a direct target of miR-509-3p

Since miR-509-3p significantly down-regulated luciferase activity and CDK2 protein expression, we examined whether down-regulation occurs *via* an interaction between miR-509-3p and predicted binding sites in the 3′-UTR of CDK2. Wild-type and mutated reporter plasmids were cotransfected with miR-509-3p, and luciferase activity was determined at 48 h post-transfection. TargetScan predicts 2 binding sites for miR-509-3p. However, we found that 1 additional site matched the seed region of miR-509-3p. Therefore, mutations were introduced into 1, 2, or all 3 putative binding sites for miR-509-3p in a luciferase-3′-UTR reporter plasmid. As seen in Fig. 1D, site-specific deletion at S1, S2, or S3 resulted in a slight increase in luciferase activity. A higher level of luciferase activity was observed when the 3′-UTR of CDK2 was mutated at 2 sites, indicating synergistic interaction between the target sites. Mutation at all 3 binding sites abolished repression by miR-509-3p. Together, these results show that miR-509-3p down-regulates CDK2 through interaction with 3 binding sites in the 3′-UTR of CDK2.

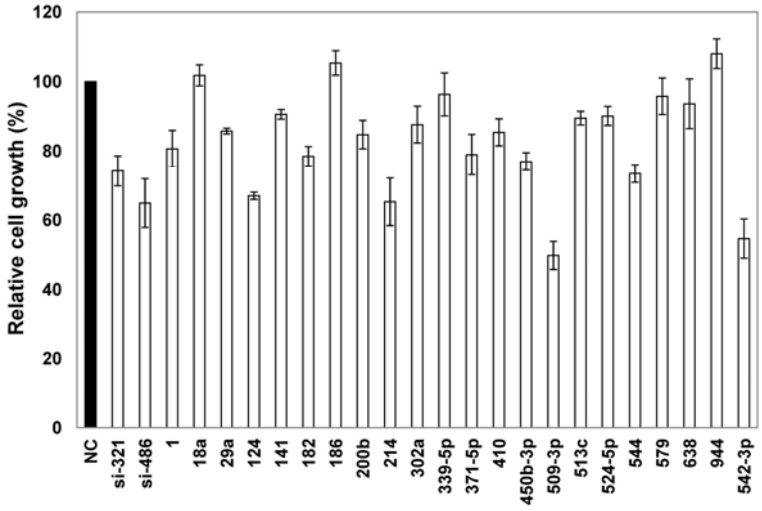

Fig. 2. Growth inhibition by miRNAs predicted to target the 3′-UTR of CDK2. A549 cells were transfected with miRNA mimics and CDK2 siRNAs (20 nM). At 72 h after transfection, cell growth was measured using CCK-8 following the manufacturer's instructions. NC was used as a negative control. The experiments were performed in triplicate and repeated twice.

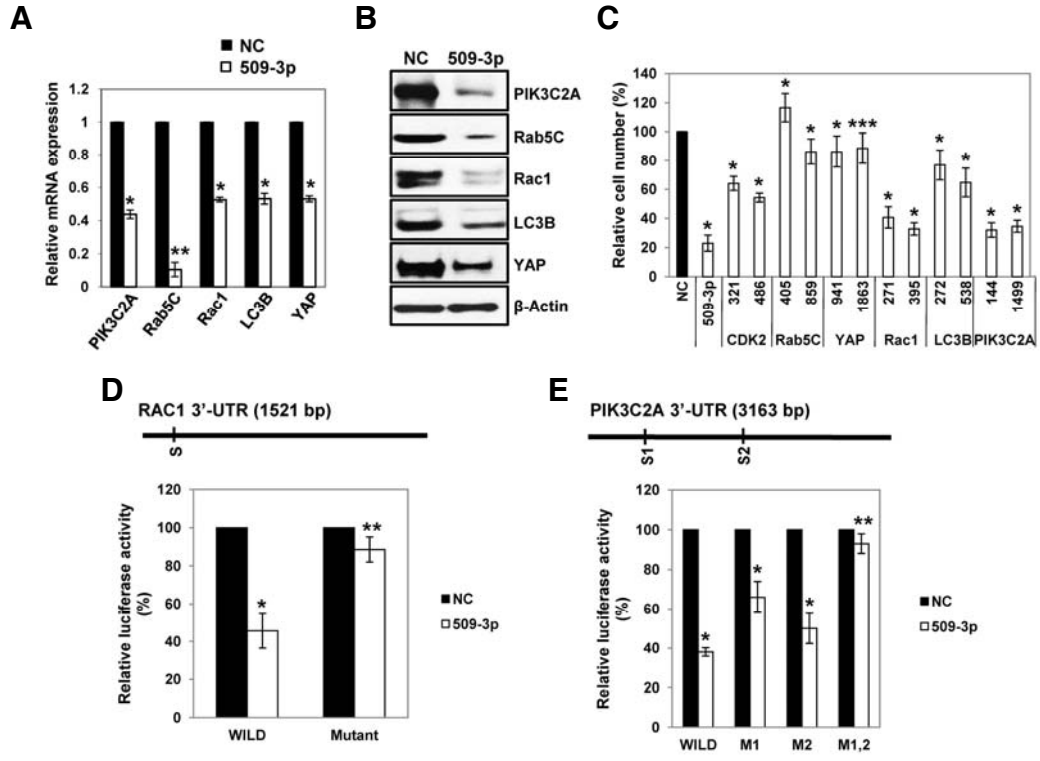

Fig. 3. Rac1 and PIK3C2A are direct targets of miR-509-3p. Decrease in the mRNA (A) and protein (B) levels of PIK3C2A, Rab5C, Rac1, LC3B, and YAP after transfection with miR-509-3p. At 24 and 48 h post-transfection, total RNA and protein were isolated and analyzed by quantitative real-time PCR and Western blot, respectively. In quantitative real-time PCR, mRNA levels in 509-3p-transfected cells are expressed as mean ± SD relative to that in NC-transfected cells, which is set to 1. GAPDH and β-actin were used as normalization (A) and loading (B) controls, respectively. $^{*}P < 0.001$, $^{**}P < 0.01$. (C) Inhibitory effects of siRNAs on cell proliferation. A549 cells were transfected with two different siRNAs for each target gene at a concentration of 20 nM. At 72 h after transfection, cells were harvested using trypsin and the total cell number was counted using a hemocytometer. Relative cell growth was determined by setting the number of NC-transfected cells at 100%. The target sequence of siRNAs used in this experiment is shown in Supplementary Table 1. $^{*}P < 0.001$, $^{***}P < 0.05$. (D) Top: A schematic diagram of a binding site (S) for miR-509-3p in the 3′-UTR of Rac1. Bottom: Direct targeting of the Rac1 3′-UTR by miR-509-3p, as revealed by the luciferase reporter assay. $^{*}P < 0.001$, $^{**}P < 0.01$. (E) Top: A schematic diagram depicting 2 binding sites (S1 and S2) for miR-509-3p in the 3′-UTR of PIK3C2A. Bottom: A luciferase reporter assay was performed 48 h after cotransfection with 10 nM of miR-509-3p and the wild-type or mutated 3′-UTR of PIK3C2A. WILD, wild-type 3′-UTR; M1, mutated at S1; M2, mutated at S2; M1, 2, mutated at S1 and S2. $^{*}P < 0.001$, $^{**}P < 0.01$.

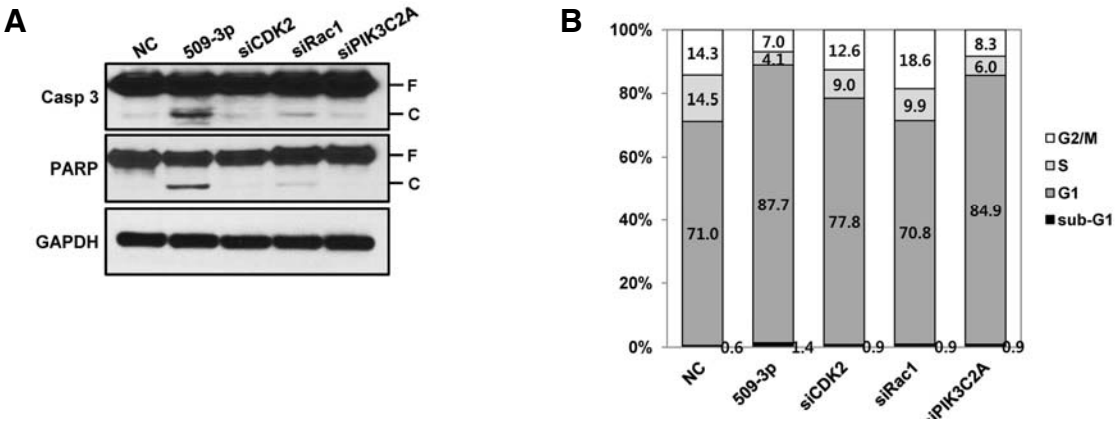

Fig. 4. Effects of miR-509-3p on apoptosis and cell cycle progression. (A) Detection of cleaved caspase 3 and PARP by Western blot analysis. At 48 h post-transfection, cells were collected, lysed, and analyzed by immunoblot. GAPDH was used as a normalization control. F, full-length protein; C, cleaved fragment. In Figs. 4, 5, and 6, CDK2-486, Rac-395, and PIK3-144 were used as siRNAs against CDK2, Rac1, and PIK3C2A, respectively. (B) Cell cycle analysis of transfected A549 cells. At 72 h post-transfection, cells were stained with propidium iodide and the cell-cycle profile was analyzed by FACS.

Growth inhibition by miRNAs that are predicted to target CDK2

Since CDK2 plays an important role in cell cycle progression, we examined the effects of miRNAs predicted to target CDK2 on the proliferation of A549 cells by CCK-8 assay. As shown in Fig. 2, variable levels of growth inhibition were observed after transfection with 22 miRNAs. Notably, the inhibition of cell growth was more pronounced in miR-509-3p-transfected cells than in CDK2-siRNA-transfected cells. Since a single miRNA can regulate tens or hundreds of target genes, these results imply that additional target(s) other than CDK2 may also affect cell proliferation. To identify targets of miR-509-3p involved in growth inhibition, we used a microarray-based approach.

Rac1 and PIK3C2A are direct targets of miR-509-3p

At 24 h after transfection, total RNAs were prepared and subjected to microarray analysis. Of the 19,070 genes analyzed, 275 transcripts were down-regulated by 2 fold or greater in cells transfected with miR-509-3p, when compared to NC-transfected cells. Among them, 117 transcripts were predicted by TargetScan to be targets of miR-509-3p. The top-ranked 20 candidate genes are shown in Supplementary Table 3, according to decreased expression levels in miR-509-3p-transfected cells. Upon close inspection of candidate target genes, we selected 5 genes for further study based on their potential effects on cell growth. Quantitative real-time PCR and Western blot analyses show that miR-509-3p reduced both the mRNA and protein levels of all 5 genes (Figs. 3A and 3B). To assess the effect on cell growth, cells were counted 72 h after transfection with 2 different siRNAs targeting each gene (see Supplementary Fig. 2 for knockdown efficiency). Figure 3C shows that cell proliferation was significantly inhibited by siRNAs against Rac1 and PIK3C2A. When using a mixture containing siRNAs against CDK2, Rac1, and PIK3C2A, the growth inhibition was comparable to that in miR-509-3p-transfected cells, indicating their additive effects on cell proliferation (data not shown). To determine whether these genes are a direct target of miR-509-3p, A549 cells were cotransfected with miR-509-3p and luciferase reporter plasmids harboring the 3′-UTR of either Rac1 or PIK3C2A. Results of the luciferase assay at 48 h post-transfection show that the luciferase activity was significantly decreased in cells transfected with reporter plasmids bearing the wild-type 3′-UTR of Rac1 or PIK3C2A, and mutation of the binding sites for miR-509-3p within the 3′-UTR abrogated the repression of luciferase activity (Figs. 3D and 3E). These results indicate that miR-509-3p down-regulates Rac1 and PIK3C2A by targeting binding sites in the 3′-UTR. It seems likely that, in addition to CDK2, inhibition of Rac1 and PIK3C2A expression contributes to the ability of miR-509-3p to inhibit cell growth in an additive and/or synergistic manner.

Effects of miR-509-3p on apoptosis, cell cycle progression, and colony formation

To determine whether miR-509-3p induces apoptosis, Annexin V staining was performed on transfected cells. Very few cells were stained at 48 h after transfection, indicating that apoptosis was not induced by miR-509-3p or siRNAs targeting CDK2, Rac1, and PIK3C2A (data not shown). Similar results were obtained by Western blot analysis using caspase 3 and PARP (its substrate) antibodies: only a very small fraction of caspase 3 and PARP was cleaved after transfection with miR-509-3p or siRNAs against CDK2, Rac1, and PIK3C2A (Fig. 4A). Since miR-509-3p did not induce apoptosis in A549 cells, we next examined the effects of miR-509-3p on cell cycle progression by flow cytometry. As shown in Fig. 4B, the percentage of miR-509-3p-transfected cells in the G1 phase was significantly increased when compared to NC-transfected cells. Similarly, a substantial number of cells accumulated in the G1 phase when transfected with siRNAs against PIK3C2A and CDK2. In contrast, there was no increase of Rac1-siRNA-transfected cells in the G1 phase, whereas the G2/M cell population was slightly increased. These results indicate that the induction of G1 arrest by miR-509-3p may be mediated by down-regulation of CDK2 and PIK3C2A. To further examine the effects of miR-509-3p on cell growth, we performed a colony formation assay. As shown in Fig. 5A and 5B, colony formation was significantly inhibited by small RNAs in the order of miR-509-3p > PIK3C2A siRNA > Rac1 siRNA > CDK2 siRNA. When transfected with a mixture

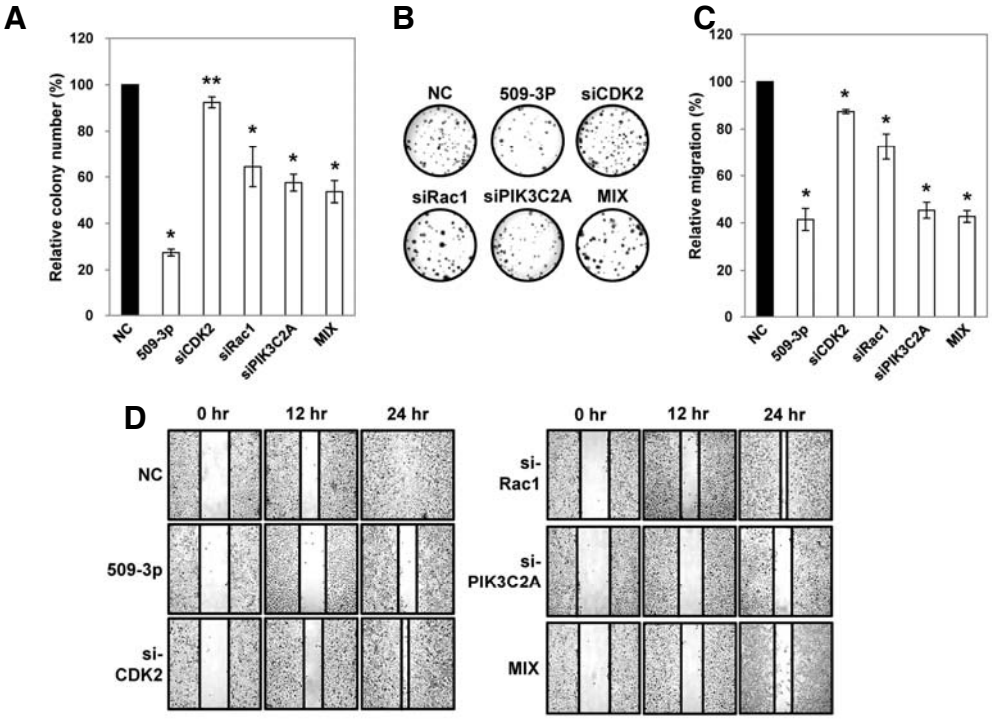

Fig. 5. miR-509-3p inhibits colony formation and migration of A549 cells. (A) Effect of miR-509-3p and siRNAs on colony-forming abilities. The relative colony formation is shown after setting the number of colonies formed from cells transfected with NC to 100%. The experiments were performed in triplicate and repeated thrice. **P* < 0.001, ***P* < 0.01. In Figs. 5A, 5B, 5C, and 5D, MIX represents transfection with siRNAs against CDK2, Rac1, and PIK3C2A as a mixture. (B) Photographs show stained colonies grown from cells transfected with miRNAs and siRNAs. (C) Cell migration was determined by scratch assay. Migration into the wound area was examined at 24 h post-scratching. Cell migration was expressed as migration relative to the migration of NC-transfected cells. **P* < 0.001. (D) Photographs were taken at 0, 12, and 24 h after scratch injury.

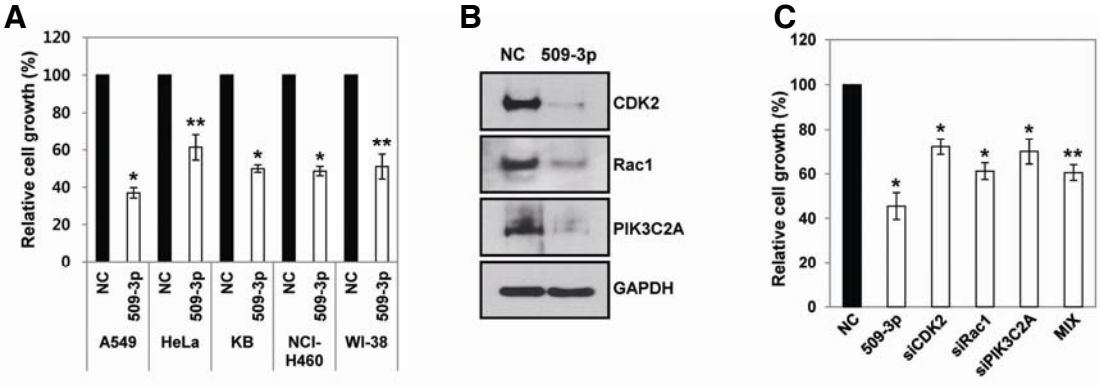

Fig. 6. Inhibition of normal and cancer cell growth by miR-509-3p. (A) A549, HeLa, KB, NCI-H460, and WI-38 cells were transfected with NC and miR-509-3p (20 nM). At 72 h after transfection, cell growth was measured by cell counting. (B) NCI-H460 cells were transfected with NC and miR-509-3p and, 48h post-transfection, total protein was isolated and analyzed by Western blotting. (C) NCI-H460 cells were transfected with siRNAs against CDK2, Rac1, and PIK3C2A and 72 h post-transfection, cell growth was measured by cell counting. NC was used as a negative control. MIX; transfection with siRNAs against CDK2, Rac1, and PIK3C2A as a mixture. **P* < 0.001, ***P* < 0.01.

containing siRNAs targeting CDK2, Rac1, and PIK3C2A, the inhibition of colony formation was slightly more effective than that by PIK3C2A-siRNA-transfected cells, although less effective than that by miR-509-3p-transfected cells. These results indicate that knockdown of CDK2, Rac1, and PIK3C2A may contribute, at least in part, to the inhibitory effect of miR-509-3p

on colony formation. These findings also suggest the possibility that additional target(s) other than CDK2, Rac1, and PIK3C2A may affect colony formation, as indicated by potent inhibition of colony formation by miR-509-3p. In addition to the inhibitory role of miR-509-3p in the growth of A549 cells, miR-509-3p suppressed the growth of other types of cancer cells including HeLa (cervical carcinoma), KB (HeLa contaminant), and NCI-H460 (lung carcinoma) (Fig. 6A). miR-509-3p also inhibited the growth of WI-38 (normal human lung fibroblast) as well as breast cancer cells such as MCF-7, SK-BR3, and BT-474, suggesting that miR-509-3p may exert its growth inhibitory effects in a wide range of cell types (Fig. 6A; data not shown). In NCI-H460 cells, CDK2, Rac1, and PIK3C2A were down-regulated by miR-509-3p and siRNAs against CDK2, Rac1, and PIK3C2A inhibited the cell growth, indicating that similar mechanisms underlie the growth inhibitory role of miR-509-3p in NCI-H460 cells (Figs. 6B and 6C).

miR-509-3p inhibits migration of A549 cells

To determine whether miR-509-3p affects cell migration, we performed an *in vitro* scratch assay. The migration of A549 cells was significantly inhibited by miR-509-3p and PIK3C2A siRNA and, to a lesser extent, by siRNAs against Rac1 and CDK2 (Figs. 5C and 5D). Knockdown of CDK2, Rac1, and PIK3C2A phenocopied the negative effect of miR-509-3p on cell migratory activity. Taken together, our results demonstrate that CDK2, Rac1, and PIK3C2A are direct targets of miR-509-3p and major contributors to miR-509-3p-mediated suppression of cell growth, colony formation, and migration in A549 cells.

In support of our finding that miR-509-3p is a growth-suppressive miRNA, several studies have demonstrated that knockdown of CDK2, Rac1, and PIK3C2A by siRNA or miRNA results in the suppression of cell growth and/or migration (Akunuru et al., 2011; Elis et al., 2008; Kang et al., 2005; Ng et al., 2009; Wu et al., 2011). In particular, among the 8 catalytic isoforms of phosphoinositide 3-kinase, down-regulation of PIK3C2A was the most effective at inhibiting cell growth. Although apoptosis was induced by knockdown of PIK3C2A in HeLa and Chinese hamster ovary cells, caspase-dependent apoptosis was not triggered by miR-509-3p or PIK3C2A siRNA in A549 cells, indicating cell type-specific differences in the activation of apoptosis (Elis et al., 2008; Kang et al., 2005). Since knockdown of PIK3C2A alone was sufficient to significantly inhibit cell growth in more than half of the 23 cell types tested (Elis et al., 2008), it is likely that miR-509-3p, which collectively down-regulates CDK2, Rac1, and PIK3C2A, exerts its growth-inhibitory effect across a wide range of cell types. Recently, it was shown that miR-509-3p inhibits renal cell growth and migration (Zhai et al., 2012). In this study, we found that CDK2, Rac1, and PIK3C2A act as key mediators in growth suppression by miR-509-3p, thus providing new insights into the molecular mechanism underlying the biological function of miR-509-3p. Consistent with its role as a growth suppressor, the expression of miR-509-3p was low in A549 cancer cells compared to that in normal human lung tissue, as assessed by real-time PCR (Supplementary Fig. 3). As a way to block several important cellular pathways, such as cell-cycle progression and migration, the addition of miR-509-3p to cancer cells may have therapeutic utility in the treatment of cancer.

Note: Supplementary information is available on the Molecules and Cells website (www.molcells.org).

ACKNOWLEDGMENTS

This work was supported by the National Research Foundation of Korea Grant funded by the Korean Government (The Ministry of Education, Science and Technology)[NRF-2010-359-C00024]. This research was also supported by Basic Science Research Program through the National Research Foundation of Korea (NRF) funded by the Ministry of Education, Science and Technology (2011-0007189).

REFERENCES

Akunuru, S., Palumbo, J., Zhai, Q.J., and Zheng, Y. (2011). Rac1 targeting suppresses human non-small cell lung adenocarcinoma cancer stem cell activity. PLoS One *6*, e16951.
Aqeilan, R.I., Calin, G.A., and Croce, C.M. (2010). miR-15a and miR-16-1 in cancer: discovery, function and future perspectives. Cell Death Differ. *17*, 215-220.
Bader, A.G. (2012). miR-34 - a microRNA replacement therapy is headed to the clinic. Front. Genet. *3*, 120.
Bartel, D.P. (2004). MicroRNAs: genomics, biogenesis, mechanism, and function. Cell *116*, 281-297.
Büssing, I., Slack, F.J., and Grosshans, H. (2008). let-7 microRNAs in development, stem cells and cancer. Trends Mol. Med. *14*, 400-409.
Choung, S., Kim, Y.J., Kim, S., Park, H.O., and Choi, Y.C. (2006). Chemical modification of siRNAs to improve serum stability without loss of efficacy. Biochem. Biophys. Res. Commun. *342*, 919-927.
Elis, W., Triantafellow, E., Wolters, N.M., Sian, K.R., Caponigro, G., Borawski, J., Gaither, L.A., Murphy, L.O., Finan, P.M., and Mackeigan, J.P. (2008). Down-regulation of class II phosphoinositide 3-kinase alpha expression below a critical threshold induces apoptotic cell death. Mol. Cancer Res. *6*, 614-623.
Faber, A.C., and Chiles, T.C. (2007). Inhibition of cyclin-dependent kinase-2 induces apoptosis in human diffuse large B-cell lymphomas. Cell Cycle *6*, 2982-2989.
He, L., and Hannon, G.J. (2004). MicroRNAs with a big role in gene regulation. Nat. Rev. Genet. *5*, 522-531.
Hermeking, H. (2010). The miR-34 family in cancer and apoptosis. Cell Death Differ. *17*, 193-199.
Hoshino, I., and Matsubara, H. (2013). MicroRNAs in cancer diagnosis and therapy: from bench to bedside. Surg. Today *43*, 467-478.
Hu, B., Mitra, J., van den Heuvel, S., and Enders, G.H. (2001). S and G2 phase roles for Cdk2 revealed by inducible expression of a dominant-negative mutant in human cells. Mol. Cell. Biol. *21*, 2755-2766.
Kang, S., Song, J., Kang, J., Kang, H., Lee, D., Lee, Y., and Park, D. (2005). Suppression of the alpha-isoform of class II phosphoinositide 3-kinase gene expression leads to apoptotic cell death. Biochem. Biophys. Res. Commun. *329*, 6-10.
Kim, S., Lee, U.J., Kim, M.N., Lee, E.J., Kim, J.Y., Lee, M.Y., Choung, S., Kim, Y.J., and Choi, Y.C. (2008). MicroRNA miR-199a* regulates the MET proto-oncogene and the downstream extracellular signal-regulated kinase 2 (ERK2). J. Biol. Chem. *283*, 18158-18166.
Long, X.E., Gong, Z.H., Pan, L., Zhong, Z.W., Le, Y.P., Liu, Q., Guo, J.M., and Zhong, J.C. (2010). Suppression of CDK2 expression by siRNA induces cell cycle arrest and cell proliferation inhibition in human cancer cells. BMB Rep. *43*, 291-296.
Ng, S.K., Neo, S.Y., Yap, Y.W., Karuturi, R.K., Loh, E.S., Liau, K.H., and Ren, E.C. (2009). Ablation of phosphoinositide-3-kinase class II alpha suppresses hepatoma cell proliferation. Biochem. Biophys. Res. Commun. *387*, 310-315.
Ortega, S., Prieto, I., Odajima, J., Martín, A., Dubus, P., Sotillo, R., Barbero, J.L., Malumbres, M., and Barbacid, M. (2003). Cyclin-dependent kinase 2 is essential for meiosis but not for mitotic cell division in mice. Nat. Genet. *35*, 25-31.
Tetsu, O., and McCormick, F. (2003). Proliferation of cancer cells despite CDK2 inhibition. Cancer Cell *3*, 233-245.
Tsai, L.H., Lees, E., Faha, B., Harlow, E., and Riabowol, K. (1993). The cdk2 kinase is required for the G1-to-S transition in mammalian cells. Oncogene *8*, 1593-1602.

Wang, X., Gorospe, M., Huang, Y., and Holbrook, N.J. (1997). p27Kip1 overexpression causes apoptotic death of mammalian cells. Oncogene *15*, 2991-2997.

Wu, L., Cai, C., Wang, X., Liu, M., Li, X., and Tang, H. (2011). MicroRNA-142-3p, a new regulator of RAC1, suppresses the migration and invasion of hepatocellular carcinoma cells. FEBS Lett. *585*, 1322-1330.

Zhai, Q., Zhou, L., Zhao, C., Wan, J., Yu, Z., Guo, X., Qin, J., Chen, J., and Lu, R. (2012). Identification of miR-508-3p and miR-509-3p that are associated with cell invasion and migration and involved in the apoptosis of renal cell carcinoma. Biochem. Biophys. Res. Commun. *419*, 621-626.